



Depósito de Investigación  
Universidad de Sevilla

Depósito de investigación de la Universidad de Sevilla

<https://idus.us.es/>

“This is an Accepted Manuscript of an article published by Elsevier in FOOD RESEARCH INTERNATIONAL on May 2024, available at: <https://doi.org/10.1016/j.foodres.2024.114242>”.



26 Brazilian cheeses. Partial least squares (PLS) regression models based on vis/NIR-HSI, NIRS,  
27 NIR-HSI data and HSI spectroscopic data fusion (vis/NIR + NIR) demonstrated excellent  
28 performance to predict moisture content ( $RPD > 2.5$ ), good ability to predict fat content ( $2.0 <$   
29  $RPD < 2.5$ ) and can be used to discriminate between high and low protein values ( $\sim 1.5 < RPD$   
30  $< 2.0$ ). The results obtained for imaging and conventional equipment are comparable and  
31 sufficiently accurate, so that both can be adapted to predict the chemical composition of the  
32 Brazilian traditional cheeses used in this study according to the needs of the industry.

33

34 **Keywords:** artisanal cheeses; denomination of origin; non-destructive technologies; visible-  
35 near infrared (vis/NIR) spectroscopy; chemometrics; data fusion.

36

## 37 **1. Introduction**

38 Historical aspects, regional characteristics, manufacturing technologies, microbial diversity  
39 and dairy species contributed to the emergence of different cheeses with unique  
40 characteristics that reflect the cultural identity of certain populations. In Brazil, there is a wide  
41 type of traditional cheeses that are part of the heritage and identity of different regions,  
42 including the North (Marajó cheese), Northeast (Butter and Coalho), South (Colonial and  
43 Serrano), Southeast (Araxá, Campo das Vertentes, Cerrado, Canastra and Serro) and Center  
44 (Caipira) of the country (Margalho et al., 2021).

45 Traditional Brazilian cheeses have gained greater visibility in recent years, especially through  
46 the granting of Geographical Indications (GI), awards in national and international  
47 competitions (such as the World Cheese Awards) and, above all, through the approval of new  
48 regulations. To date, five geographical indications have been granted in the Indication of  
49 Origin (IP) modality, which recognizes the traditional area of cheese production, historical  
50 connotation and economic relevance (Serro, Canastra, Colônia Witmarsum, Marajó and

51 Cerrado); and a GI in the Denomination of Origin (DO) modality, which recognizes the  
52 specificities of the geographic environment, including natural factors (suitable climate and  
53 native pastures) and human factors, which provide the product with unique characteristics (the  
54 terroir, such as Serrano cheese “Campos de Cima da Serra”) (Brasil, 1996a). In 2018, through  
55 new regulations, the “Arte” seal was created, which now allows the retail sale of artisanal  
56 cheeses made with raw milk throughout the national territory (Brasil, 2018).

57 The GIs and the “Arte” seal connect characteristic cheeses to their place of origin and,  
58 through know-how passed down through generations, recognizes their own identity and adds  
59 value, which increases the interest of other producers in regulating their products.  
60 Consequently, it is necessary to know the characteristics of artisanal cheeses and identify  
61 markers that can assist in the certification of products with geographical indication and in the  
62 identification of fraudulent products (Santos et al., 2017).

63 Different methodologies based on chemical composition (Fitztum et al., 2023; Santos et al.,  
64 2017) and gas chromatograph (Margalho et al., 2021), Mid-Infrared Spectroscopy (MIR),  
65 Reversed-Phase High Performance Liquid Chromatography (RP-HPLC) (Silva et al, 2023),  
66 and inductively coupled plasma optical emission spectrometer (ICP-OES) (Andrade et al.,  
67 2022) were applied to characterize and discriminate cheeses according to the type or region of  
68 production. Despite presenting promising results, it is necessary to investigate new techniques  
69 that allow obtaining reliable, fast, and low-cost results.

70 Techniques based on vibrational spectroscopy in the visible/near infrared range (vis/NIR)  
71 have consolidated applications in the food industry (Ayvaz et al., 2021; Stocco et al., 2019;  
72 Wiedemair et al., 2019; Marinoni et al., 2017; Madalozzo et al., 2015; Karoui et al., 2006;)  
73 and has been investigated as a tool for authentication. Vis/NIR spectroscopy provides a  
74 spectrum of the sample, often called “fingerprint”, which can be used to extract information  
75 related to its composition. It is characterized as being non-destructive, avoiding the use of

76 chemicals and allowing rapid characterization and measurement of several attributes  
77 simultaneously at any stage of the production chain and directly on the surface of the cheese.  
78 However, the potential of vis/NIR can be compromised in heterogeneous matrices, such as  
79 ripened cheeses, as conventional spectrometers provide information from a small portion of  
80 the sample. To overcome this difficulty, it is possible to use vis/NIR hyperspectral imaging  
81 (HSI), which combines in a single device the advantages of conventional spectroscopy and  
82 artificial vision, allowing the simultaneous acquisition of information related to composition  
83 (spectral information) and its distribution within the sample (spatial information) (Amigo et  
84 al., 2019). Considering the shortages of studies in this field, there is a need for further  
85 investigation comparing the application of hyperspectral imaging and conventional  
86 spectrometers to predict the composition of a wider type of cheeses and without the need for  
87 sample preparation.

88 Due to the large amount of information generated by hyperspectral imaging and conventional  
89 spectroscopy, a data mining step (also known as chemometrics) becomes necessary to extract  
90 only the relevant information from spectra. Spectral pre-processing steps are performed to  
91 remove/minimize the influence of undesirable phenomena that affect the spectral  
92 measurement, such as light scattering, particle size and morphology effects and detector  
93 artifacts. However, there is no standard method, and a trial-and-error approach is required for  
94 a specific application. Additionally, a wavelength selection step can be performed to develop  
95 simpler models, reducing data processing time and allowing industrial applications (Pasquini,  
96 2018; Amigo, 2019). Finally, algorithms are applied to investigate spectral variability and  
97 develop models to predict chemical compounds of interest.

98 Thus, this study compared the performance of NIRS and hyperspectral imaging (vis/NIR-HSI  
99 and NIR-HSI) devices, as well as the fusion of HSI spectroscopic data (vis/NIR + NIR) to  
100 discriminate and predict the chemical composition of a wide type of Brazilian traditional

101 cheeses. In this work, we investigate the relationship of cheese processing steps with spectral  
 102 variability, and the influence of instrument technology (image and point measurement),  
 103 spectral region (vis and NIR) and spectral preprocessing methods on the performance of  
 104 classification and predictive models.

105

## 106 2. Material and methods

### 107 2.1. Brazilian traditional cheese samples

108 Seventy-two samples of seven types of Brazilian traditional cheeses were obtained from  
 109 producers, supermarkets and markets located in three regions of Brazil were analyzed:  
 110 Northeast, Southeast and South. The sample set (Table 1) included the main types of  
 111 traditional Brazilian cheeses and considered different production technology, curd heat  
 112 treatment (uncooked and cooked), curd melting, maturation (ripened or not ripened), chemical  
 113 composition and structural characteristics of the cheese matrix (soft and hard cheeses) to  
 114 address a wider sample variation and allow effective evaluation of the ability of vis/NIR  
 115 devices to predict chemical composition.

116

117 **Table 1.** Description of the Brazilian traditional cheeses included in the sampling.

Region	Cheese type (Identification)	Production aspects		Regulatory patterns
		Production technology	Distinctive steps	
Northeast	Coalho integral (CO) and light (CL)	Enzymatic coagulation, cutting, stirring, whey drainage, cooking (45–55 °C), and pressing	Not ripened	Moisture: 36.0 –54.9%; FTS: 35.0 a 60.0% <sup>1</sup>
	Butter cheese integral (BC) and light (BL)	Spontaneous coagulation, desorption, washing with water and/or milk and melting (at 85°C for at least 15 min) with butteroil	Melted	Moisture: ≤54.9 %; FTS: 25.0 – 55.0% <sup>1</sup>
	Minas Frescal (MF)	Enzymatic coagulation, supplemented or not with the action of lactic acid bacteria, whey drainage and packaging	Not ripened	Moisture: >55.0%; FTS: 25.0 – 44.9% <sup>2</sup>
South/ Southeast	Minas Araxá (AR)	Coagulation with endogenous culture and industrial rennet, cutting, agitation, molding, and superficial salting. The cheese is turned daily during shelf maturation	Ripened (14 days)	Moisture: ≤ 45.9% <sup>3</sup>
	Minas Canastra (CT)	Coagulation with natural dairy culture and industrial rennet, cutting, stirring, molding, pressing, and salting	Ripened (14 days)	Moisture: ≤ 45.9% <sup>3</sup>

Minas Padrão (light) (MP)	Enzymatic coagulation, complemented by the action of lactic acid bacteria, heating (32–42°C), draining, pressing, and salting	Ripened (20 days)	Moisture: 36 a 45.9%. FTS: 42 a 57% <sup>4</sup>
Colonial (CN)	Coagulation with industrial rennet, heating (30–45°C), whey drainage, molding, pressing, and salting	Ripened (10 days)	Moisture: 36.0 a 45.9%; FTS 45.0 a 59.9% <sup>5</sup>

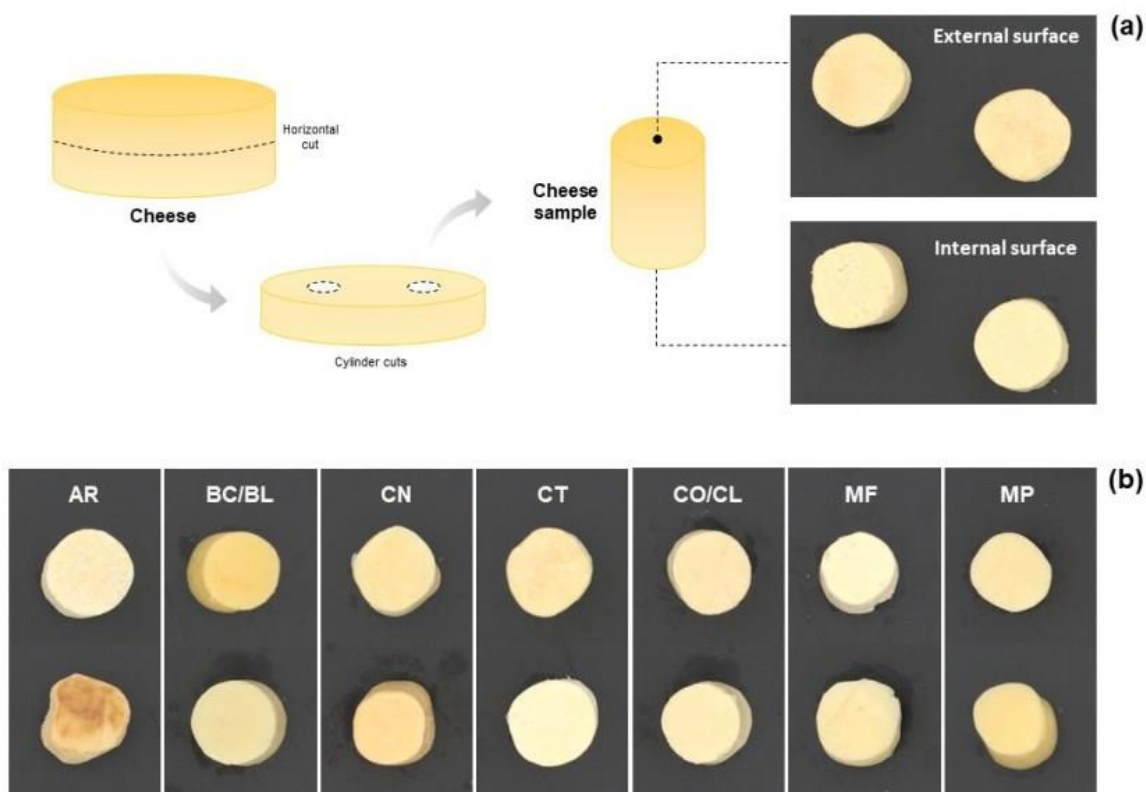
118 <sup>1</sup>Brasil (2001), <sup>2</sup>Brasil (1997), <sup>3</sup>Minas Gerais (2008), <sup>4</sup>Brasil (2020), <sup>5</sup>Rio Grande do Sul (2023).

119

## 120 2.2. Image and spectral data collection

### 121 2.2.1. Sample treatment and morphological features

122 To investigate the spectral changes associated with the cheese process, especially ripening,  
 123 the cheeses were sectioned horizontally (20 mm in height) and two cylinder of 25 mm in  
 124 diameter were removed from the center (internal surface) towards the rind (external surface),  
 125 with the aid of a stainless-steel sampler.



126

127 **Fig. 1.** Representation of obtaining cheese samples for spectral acquisition (a) and the types of  
 128 traditional Brazilian cheeses (b) included in the sampling.

129

130 **2.2.2. Portable NIR spectrometer (NIRS)**

131 Spectra were recorded using a portable NIR spectrophotometer (MicroNIR Pro Lite 1700,  
132 VIAVI, Santa Rosa, California, USA), previously calibrated, scanning the wavelength range  
133 of 908 and 1676 nm (spectral resolution of 6.2 nm). Reflectance spectra were corrected by  
134 means of a two-point calibration. For that, a white reference spectrum (Spectralon, Labsphere  
135 Inc., North Sutton, USA) and a dark current spectrum were acquired in each collection  
136 session. Finally, two spectra were acquired at random locations on the outer surface (totaling  
137 144 spectra) and two spectra on the inner surface (totaling 144 spectra) of each cheese  
138 cylinder.

139

140 **2.2.3. Hyperspectral imaging (HSI)**

141 Hyperspectral images of Brazilian traditional cheeses were acquired in the visible and near  
142 infrared spectral region (vis/NIR – HSI) using a Specim IQ camera (Spectral Imaging Ltd.,  
143 Oulu, Finland) with a spectral range of 397 to 1004 nm (512 × 512 pixels and FWHM of 7  
144 nm). This camera is based on the pushbroom principle and has a mobile, portable, and  
145 autonomous design (integrated operating system and controls), which allows the acquisition  
146 of images in different environments. This camera has a certified reflectance device made of  
147 teflon to perform the calibrations. Also, near-infrared (NIR – HSI) hyperspectral images were  
148 acquired using a laboratory system composed of a Xenics® XEVA-USB InGaAs camera (320  
149 × 256 pixels; Xenics Infrared Solutions, Inc., Leuven, Belgium), a spectrograph (Specim  
150 ImSpector N17E Enhanced; Spectral Imaging Ltd., Oulu, Finland) covering the spectral range  
151 between 884 – 1717 nm (3.25 nm spectral resolution), a mirror scanner (Spectral Imaging  
152 Ltd., Oulu, Finland) and a computer system with instrumental acquisition software  
153 SpectralDAQ v. 3.62 (Spectral Imaging Ltd., Oulu, Finland). A “white reference” image (W,  
154 100% reflectance) was acquired from a white ceramic tile (Labsphere Inc., North Sutton,



155 USA), and a “dark reference” image (B, 0% reflectance) was obtained with the light source  
156 off and the camera covered with its opaque cap.

157 The cheese cylinders were placed on a dark surface and illuminated by two 70 W tungsten  
158 iodine halogen lamps (Prilux ®, Barcelona, Spain) separated 50 cm and oriented at 45° from  
159 the area of image. The distance between the camera and the sample was 45 cm. The camera  
160 covers an angle of 24° with a speed of 5.6 degrees/sec. For each cheese cylinder, an image of  
161 the outer surface and one of the inner surfaces was recorded. After the calibration and  
162 segmentation processes, the average spectra of the region of interest (ROI) were extracted  
163 using Matlab (R2019; Mathworks, Natick, USA).

164

#### 165 **2.2.4. HSI spectroscopic dataset fusion**

166 Given the complementary nature of the information provided by the visible (vis) and near  
167 infrared (NIR) spectra, the average vis/NIR-HSI (397 to 1004 nm) and NIR-HSI (884 to 1717  
168 nm) spectra were sectioned at the 950 nm wavelength and unified into a new matrix (397 to  
169 1717 nm) to increase reach and improve classification and prediction models.

170

### 171 **2.3. Chemical composition, colorimetric parameters, and texture**

#### 172 **2.3.1. Chemical composition**

173 The samples were crushed until obtaining a homogeneous state and then were subjected to the  
174 following analyses (g/100 g of cheese): moisture, fat, proteins, and ash, according to the  
175 Association of Official Analytical Chemists protocols (AOAC, 2012). After, fat was  
176 calculated in dry matter (g/100g) for comparison with the legislation and carbohydrates were  
177 calculated by subtracting the moisture, fat, protein, and ash contents from the total  
178 composition (100%).

179 The results of moisture (g/100g of cheese) and fat in dry matter (FDM) (g/100g of dry matter)  
180 were used to classify the cheeses according to the Brazilian legislation (Brasil, 1996b), in  
181 cheeses of low (moisture < 35.9%), medium (36.0 – 45.9%), high (46.0 – 54.9%) and very  
182 high moisture (> 55.0%); and in skimmed (fat < 10.0%), low fat (10.0 – 24.9%), semi-fat  
183 (25.0 – 44.9%), full fat (45.0 – 59.9%) or extra fat (> 60%).

184

### 185 **2.3.2. Fatty acids**

186 For the quantification of fatty acid methyl esters, the sample preparation used were the same  
187 as those reported by Sant'Ana et al. (2019). The identification and quantification of fatty acid  
188 methyl esters was performed with a gas chromatograph equipped with flame ionization  
189 detection (GC-FID) (QP2010-plus, Shimadzu, Kyoto, Japan) and a fused silica capillary  
190 column (SP-2560, 100 m × 0.25 mm × 0.20 µm, Supelco, Bellefonte, PA, USA). The injector  
191 and detector were kept at 250 and 280 °C, respectively. The temperature program was as  
192 follows: 50 °C for 1 min; ramped to 150 °C at 50 °C/min and held for 20 min; then ramped to  
193 190 °C at 1 °C/min, held for 1 min; and ramped to 220 °C at 2 °C/min, held for 30 min.  
194 Helium was used as the carrier gas at 1 mL/min constant flow rate, and 1 µL of the sample  
195 was injected.

196 The identification of peaks of fatty acid methyl esters was performed by comparing the  
197 retention times with the standards (FAME Mix, 37 components) under the same analysis  
198 conditions.

199

### 200 **2.3.3. Instrumental color**

201 Instrumental color was determined by measuring the coordinates L\* (lightness), a\* (greenish  
202 for negative and reddish for positive values) and b\* (bluish for negative and yellowish for  
203 positive values), using a digital colorimeter (CM-2600D, illuminant D65 Konica Minolta

204 Sensing Inc., Osaka, Japan), calibrated with a white ceramic standard. Then, the chroma ( $C_{ab}^*$ )  
205 was calculated, which corresponds to the saturation or intensity of the color, and hue angle  
206 ( $h_{ab}$ ), according to CIE (1978). The Yellowness index (YI) of the samples was calculated  
207 using Equation (1) (Francis & Clydesdale, 1975).

$$208 \qquad \qquad \qquad YI = 142.86 \frac{b^*}{L^*} \qquad \qquad \qquad \text{Equation (1)}$$

209

### 210 **2.3.4. Statistical analysis**

211 One-way Analysis of Variance (ANOVA) was applied to chemical composition and  
212 instrumental color parameters to identify whether they influenced by cheese types. Tukey's  
213 multiple mean comparison test ( $p < 0.05$ ) was applied to identify differences between cheese  
214 types, using Sisvar software version 5.7 (Lavras, Minas Gerais, Brazil).

215

## 216 **2.4. Multivariate analysis**

### 217 **2.4.1. Spectral preprocessing**

218 Different pre-processing methods were applied to the vis/NIR spectra to correct effects of the  
219 random noise, light scattering, and changes in the baseline. Savitzky-Golay smoothing (SG),  
220 Standard Normal Variate (SNV) and Savitzky-Golay derivatives (1<sup>st</sup> SG and 2<sup>nd</sup> SG) (both  
221 derivatives were used with a 13-point window and second order polynomial filtering) were  
222 tested alone or in combinations (SG + SNV, SNV + 1<sup>st</sup> SG and SNV + 2<sup>nd</sup> SG). The best  
223 results obtained for each equipment and chemical component are presented in the results. All  
224 pre-processing and post analysis were performed using PLS Toolbox 8.9.1 from Eigenvector  
225 Research, Inc. (Manson, WA, USA) to Matlab R2019a (Mathworks, Natick, USA).

226

### 227 **2.4.2. Principal Component Analysis (PCA)**

228 Principal Component Analysis (PCA) was initially performed to investigate the influence of  
229 the spectral acquisition surface (external and internal surface of the cheese) on the grouping of  
230 cheeses. It was observed that both surfaces allow visualization of groupings between samples  
231 and explain close variance percentages. Thus, the external surface spectra (144 spectra, two  
232 for each sample) were chosen for the PCA and other multivariate analyzes for maintaining the  
233 integrity of the samples and the non-destructive nature of the spectroscopic method. Finally,  
234 Principal Component Analysis (PCA) was applied to the complete spectra and informative  
235 region (spectrum region with peaks and absorption differences between samples) to  
236 investigate spectral variability of the cheeses and correlate the grouping of samples with the  
237 cheese type, differences between the chemical composition and distinctive steps related to  
238 production (ripening, curd heating and curd melting). PCA models were developed using  
239 singular value decomposition (SVD) algorithm (95% confidence level) and outliers were  
240 detected and eliminated using Hotelling's residual Q and  $T^2$  values.

241

### 242 **2.4.3. Classification and prediction models**

243

244 Classification models based on the Partial Least Squares Discriminant Analysis (PLSDA)  
245 method were constructed to discriminate the seven types of traditional Brazilian cheeses.  
246 Furthermore, regression models (PLSR) were built to predict the chemical composition of the  
247 cheeses: moisture, fat, proteins, and ash.

248 Initially, the classification and prediction models were developed using the full spectrum and  
249 then a variable selection step was applied to build reduced models. Selection of optimal  
250 wavelengths was performed by two approaches: (1) Informative region and (2) Interval Partial  
251 Least Squares algorithm (iPLS). The selection of the informative region was performed by  
252 visual inspection of the spectrum, considering regions with higher peaks and differences

253 between cheese samples. For the vis/NIR-HSI data, the spectrum was divided into two  
254 informative regions: 387 – 780 nm (visible region) and 780 – 1004 nm (infrared region); and  
255 in the NIRS and NIR-HSI data, were studied the regions of 1100 – 1600 nm and 1050 – 1350,  
256 1600 – 1680 nm (Medeiros et al, 2023). The iPLS was performed considering one wavelength  
257 per interval and limited to 10 intervals. In addition to the classification models based on  
258 spectral information, a model based on chemical composition was built to compare the  
259 efficiency of spectral techniques with traditional chemical methods.

260 In both models, 70% of the samples (50 samples) were used and the remaining 30% (22  
261 samples), containing at least two samples of each cheese type, were used as an independent  
262 set to test the predictive capacity of the models. The optimal number of latent variables (LV)  
263 in the classification and prediction models was chosen using the lowest average classification  
264 error in cross-validation (leave-one-out) and lowest root mean squared error of cross  
265 validation (leave-one-out) (RMSECV), respectively.

266 The performance of PLS-DA models was evaluated by sensitivity (fraction of samples that  
267 belong to a class and are properly accepted) (Eq. (1)), specificity (fraction of samples that do  
268 not belong to a class and are correctly rejected) (Eq. (2)), accuracy (ratio between the number  
269 of samples correctly classified, regardless of the class, and the total number of samples) (Eq.  
270 (3)) and error (Eq. (4)).

271 
$$\text{Sensitivity} = \frac{TP}{TP + FN} \quad (\text{Eq. 1})$$

272 
$$\text{Specificity} = \frac{TN}{FP + TN} \quad (\text{Eq. 2})$$

273 
$$\text{Accuracy} = \frac{TP + TN}{TP + TN + FP + FN} \times 100 \quad (\text{Eq. 3})$$

274 
$$\text{Error} = \frac{FP + FN}{TP + FP + TN + FN} \times 100 \quad (\text{Eq. 4})$$

275

276 where TP is true positive, TN is true negative, FN is false negative, and FP is false positive.

277 The performance of the calibration models was evaluated by the coefficient of determination  
278 ( $R^2$ ) and Root Mean Square Error (RMSE) for the calibration ( $R_C^2$ , RMSEC) and cross-  
279 validation ( $R_{CV}^2$ , RMSECV) and the predictive capacity of the models was evaluated using the  
280 coefficient of determination ( $R_P^2$ ), Root Mean Square Error (RMSEP) and Performance Ratio  
281 to Deviation (RPD = SD/RMSEP, where SD is the standard deviation of the chemical  
282 component content) (Nicolai et al., 2007).

283

### 284 **3. Results and discussion**

#### 285 **3.1. Chemical composition and instrumental color parameters**

286 Brazilian traditional cheeses showed significant differences ( $p < 0.05$ ) for the evaluated  
287 compositional parameters (Table 1): Moisture (34.35 – 54.43%), fat (9.07 – 36.47%), fat in  
288 total solids (17.50 – 55.88%), protein (18.78 – 28.35%), carbohydrates (0.39 – 10.19%) and  
289 ash (1.64 – 5.45%).

290 The main differences for moisture content were observed for Minas Canastra (CT), which had  
291 the lowest moisture content. This cheese undergoes a minimum maturation period of 14 days,  
292 where a series of biochemical events take place, responsible for its flavor and texture, as well  
293 as for the reduction of moisture. The highest moisture contents were observed for light butter  
294 cheese (BL), Minas Frescal (MF) and Minas Padrão light (MP) cheeses. MF cheese is  
295 characterized by being marketed fresh (not matured), and BL and MP cheeses are  
296 characterized by a reduction in fat content, implying an increase in moisture content.  
297 According to Brazilian legislation (Brasil, 1996b), the analyzed cheeses are classified as low  
298 cheeses (hard cheeses) ( $< 35.9\%$ ) to high cheeses (soft cheeses) (46.0 – 54.9%) moisture  
299 content and comply with their respective technical regulations.

300 The lowest levels of fat were observed for BL and MP cheese (11.48 and 13.51%), while the  
301 highest fat content was observed for BC cheese (29.25%). These differences are mainly

302 attributed to the ingredients used during cheese production. Although these cheeses are  
303 produced from skimmed milk, butter cheese has as its main characteristic the addition of  
304 butteroil during the melting process of the coagulated mass. This butter, typical of the  
305 northeast region of Brazil, is obtained by heating cream (110 to 120°C) until complete  
306 melting and contains a minimum fat content of 98.5%, contributing to a higher fat content in  
307 the butter cheese. According to the fat content in the dry extract, the analyzed cheeses are  
308 classified between lean (10–24.9 %) and full fat (45–59.9 %) (Brasil, 1996b) and are in  
309 accordance with the provisions of their respective technical regulations.

310 The main difference in protein content was observed for MP cheese (27.31%) (highest  
311 content) and is related to the incorporation of whey protein concentrate, which is used to  
312 improve the yield or sensory properties of low-fat cheeses. All other cheeses had protein  
313 contents between 22.74 and 24.96% and are in line with reports by other authors (Costa et al.,  
314 2022; Margalho et al., 2021).

315 The lowest carbohydrate contents were observed for matured cheeses (Minas - Canasta and  
316 Colonial) (2.15 – 2.84%) and for Coalho cheese (2.58%). The amount of carbohydrates in the  
317 cheese is influenced by the concentration of lactose in the milk, type and amount of coagulant,  
318 as well as aspects related to the curd washing step, such as washing time, amount of water and  
319 particle size (Hayaloglu & McSweeney, 2014; Ibáñez et al., 2020). In addition, in mature  
320 cheeses, lactose is metabolized by lactic acid bacteria, releasing glucose and galactose, and  
321 synthesizing organic acids, resulting in low carbohydrate content (Bezerra et al., 2017). The  
322 highest carbohydrate contents were observed for light cheeses (BL, MP and CL) (4.82 to  
323 8.66%). This result can be attributed to the lower fat content present in these cheeses, which  
324 consequently alters the amount of other constituents.

325 The main differences in ash content were observed for butter cheese (BC and BL) (2.11 and  
326 2.60%) and CL (4.18%) and may be related to some particular steps during manufacture of

327 these cheeses. In butter cheese, the milk is coagulated by the action of acids and then  
328 subjected to draining, washing, and melting with butteroil. Acid coagulation causes colloidal  
329 calcium phosphate solubilization (Masotti et al., 2020) and washing can promote the leaching  
330 of minerals into the whey, contributing to the reduction of mineral content. On the other hand,  
331 in the production of CO cheese, as well as in CL, MP and MF cheeses, calcium chloride is  
332 added as an ingredient to provide ideal conditions for milk coagulation (improves gel  
333 firmness and reduces coagulation time), resulting in an increase in mineral content (Koutina et  
334 al., 2016). Minas traditional AR and CT cheeses had statistically equal mineral contents ( $p <$   
335  $0.05$ ) to cheeses with added calcium chloride. Although these cheeses do not have addition of  
336 calcium chloride, this increase may be related to differences in the percentage of salt added in  
337 the technological process and the concentration of solids during maturation.

338 The composition intervals presented in this study are in accordance with those reported by  
339 Margalho et al. (2021) for 402 samples of 11 types of Brazilian artisan cheeses and are close  
340 to those reported by authors who obtained robust models to predict compositional attributes in  
341 a wide type of cheeses (Ayvaz et al., 2021; Stocco et al., 2019). Thus, it can be inferred that  
342 the sampling used in this study and the models developed from these data are representative  
343 of the compositional variability of Brazilian traditional cheeses.



344 **Table 2.** Chemical composition, instrumental color parameters and yellowness index (YI) of Brazilian traditional cheeses.

Region	Cheese samples	Chemical composition (%)					Color parameters (CIELAB units)				
		Moisture	Fat	FDM	Protein	Carb	Ash	L*	C <sub>ab</sub> *	h <sub>ab</sub>	YI
Northeast	Coalho - Integral (CO)	45.46 <sup>bc</sup> ± 2.62	23.34 <sup>bc</sup> ± 2.17	42.73 <sup>ab</sup> ± 2.42	24.73 <sup>ab</sup> ± 1.12	2.58 <sup>de</sup> ± 1.46	3.89 <sup>ab</sup> ± 0.66	89.1 <sup>ab</sup> ± 1.5	25.3 <sup>ab</sup> ± 2.8	100.2 <sup>ab</sup> ± 1.0	40.6 <sup>abc</sup> ± 4.7
	Coalho - Light (CL)	44.78 <sup>bcd</sup> ± 2.83	21.98 <sup>c</sup> ± 6.29	39.38 <sup>b</sup> ± 9.41	24.23 <sup>b</sup> ± 1.77	4.82 <sup>b</sup> ± 1.39	4.18 <sup>a</sup> ± 0.62	90.9 <sup>a</sup> ± 0.6	22.5 <sup>ab</sup> ± 2.2	90.8 <sup>d</sup> ± 0.5	35.4 <sup>bc</sup> ± 3.4
	Minas Frescal (MF)	46.65 <sup>b</sup> ± 2.33	22.95 <sup>bc</sup> ± 0.61	43.12 <sup>ab</sup> ± 2.87	22.74 <sup>b</sup> ± 2.43	4.42 <sup>bc</sup> ± 0.90	3.25 <sup>bc</sup> ± 0.21	90.8 <sup>a</sup> ± 4.9	20.4 <sup>b</sup> ± 2.2	98.4 <sup>bc</sup> ± 5.3	31.8 <sup>c</sup> ± 4.5
	Butter cheese - Integral (BC)	40.71 <sup>cd</sup> ± 3.84	29.25 <sup>a</sup> ± 4.57	49.06 <sup>a</sup> ± 4.66	24.56 <sup>b</sup> ± 1.24	3.36 <sup>bcd</sup> ± 1.01	2.11 <sup>d</sup> ± 0.31	69.3 <sup>d</sup> ± 4.9	25.9 <sup>ab</sup> ± 6.4	105.0 <sup>a</sup> ± 2.5	51.6 <sup>a</sup> ± 12.6
	Butter cheese - Light (BL)	54.45 <sup>a</sup> ± 0.15	11.48 <sup>d</sup> ± 0.12	25.19 <sup>c</sup> ± 0.28	23.72 <sup>b</sup> ± 0.24	7.76 <sup>a</sup> ± 0.32	2.60 <sup>cd</sup> ± 0.02	67.4 <sup>d</sup> ± 2.6	21.1 <sup>ab</sup> ± 0.7	96.7 <sup>bc</sup> ± 0.7	44.5 <sup>abc</sup> ± 3.3
South/ Southeast	Minas Araxá (AR)	42.54 <sup>bcd</sup> ± 2.27	26.78 <sup>abc</sup> ± 1.73	46.65 <sup>a</sup> ± 3.07	23.11 <sup>b</sup> ± 2.21	3.93 <sup>bcd</sup> ± 0.69	3.64 <sup>ab</sup> ± 0.36	81.2 <sup>bc</sup> ± 10.3	27.3 <sup>a</sup> ± 6.9	90.6 <sup>d</sup> ± 8.3	49.7 <sup>ab</sup> ± 19.9
	Minas Canastra (CT)	40.12 <sup>d</sup> ± 4.90	28.12 <sup>ab</sup> ± 3.47	46.86 <sup>a</sup> ± 2.83	24.96 <sup>ab</sup> ± 2.20	2.84 <sup>cde</sup> ± 0.94	3.95 <sup>ab</sup> ± 0.86	83.2 <sup>abc</sup> ± 7.9	19.7 <sup>b</sup> ± 2.3	95.9 <sup>bcd</sup> ± 2.9	33.9 <sup>c</sup> ± 5.7
	Minas Padrão light (MP)	46.55 <sup>b</sup> ± 1.10	13.51 <sup>d</sup> ± 3.37	25.17 <sup>c</sup> ± 5.86	27.31 <sup>a</sup> ± 0.96	8.66 <sup>a</sup> ± 1.45	3.98 <sup>ab</sup> ± 0.27	79.6 <sup>c</sup> ± 1.7	22.8 <sup>ab</sup> ±	94.2 <sup>cd</sup> ± 0.9	40.2 <sup>abc</sup> ± 5.6
	Colonial (CN)	43.87 <sup>bcd</sup> ± 2.14	26.29 <sup>abc</sup> ± 3.27	45.82 <sup>a</sup> ± 3.89	24.30 <sup>b</sup> ± 1.26	2.15 <sup>e</sup> ± 1.51	3.89 <sup>ab</sup> ± 0.44	83.8 <sup>abc</sup> ± 1.9	3.2	97.8 <sup>bc</sup> ± 3.8	43.3 <sup>abc</sup> ± 9.2
								25.6 <sup>ab</sup> ± 4.7			
	Range	34.35 – 54.43	9.07 – 36.47	17.50 – 55.88	18.78 – 28.35	0.39 – 10.19	1.64 – 5.45	60.9 – 94.7	17.0 – 38.5	77.2 – 109.5	26.1 – 82.4

345 FDM = Fat in dry matter and Carb = Carbohydrate. Values in the same column followed by different letters are significantly different by ANOVA test (p < 0.05).

346

347 **Table 3.** Fatty acids profile of Brazilian traditional cheeses.

Region	Cheese samples	Fatty acids profile (%)									
		C14:0	C16:0	C16:1	C18:0	C18:1	C18:2	C18:3	SFAs	MUFAs	PUFAs
Northeast	Coalho - Integral (CO)	Colonial	10.66 <sup>ab</sup> ± 1.10	10.35 <sup>ab</sup> ± 0.4	31.19 <sup>bc</sup> ± 2.35	32.91 <sup>abc</sup> ± 0.85	1.33 <sup>b</sup> ± 0.70	2.94 <sup>ab</sup> ± 1.09	13.55 <sup>ab</sup> ± 1.37	12.02 <sup>bcd</sup> ± 0.59	29.24 <sup>ab</sup> ± 2.8
	Coalho - Light (CL)	(CN)	10.65 <sup>ab</sup> ± 0.76	9	31.41 <sup>bc</sup> ± 0.16	27.05 – 38.30	1.50 <sup>b</sup> ± 0.98	0.81 – 5.04	13.33 <sup>ab</sup> ± 0.84	8.32 – 16.66	3
	Minas Frescal (MF)	Range	11.58 <sup>ab</sup> ± 1.79	8.36 –	32.73 <sup>abc</sup> ± 2.54		2.41 <sup>ab</sup> ± 1.32		12.51 <sup>abc</sup> ± 1.55		28.61 <sup>ab</sup> ± 1.9
	Butter cheese - Integral (BC)		9.77 <sup>b</sup> ± 1.10	13.15	29.22 <sup>c</sup> ± 1.62		1.71 <sup>ab</sup> ± 1.12		14.65 <sup>a</sup> ± 1.65		6
	Butter cheese - Light (BL)		11.02 <sup>ab</sup> ± 0.09		31.85 <sup>abc</sup> ± 0.01		1.17 <sup>b</sup> ± 0.04		13.77 <sup>ab</sup> ± 0.07		25.76 <sup>bc</sup> ± 3.8
South/ Southeast	Minas Araxá (AR)		12.07 <sup>a</sup> ± 0.85		36.08 <sup>a</sup> ± 2.39		1.93 <sup>ab</sup> ± 1.02		11.69 <sup>bcd</sup> ± 0.80		3
	Minas Canastra (CT)		11.95 <sup>a</sup> ± 0.57		33.56 <sup>ab</sup> ± 3.38		2.82 <sup>ab</sup> ± 1.31		9.82 <sup>d</sup> ± 1.53		30.67 <sup>a</sup> ± 2.97
	Minas Padrão light (MP)		11.03 <sup>ab</sup> ± 0.78		32.85 <sup>abc</sup> ± 1.80		3.60 <sup>a</sup> ± 1.27		10.55 <sup>cd</sup> ± 0.56		29.33 <sup>ab</sup> ± 0.0

4	22.60 <sup>c</sup> ±2.56	2.32 <sup>ab</sup> ±0.23	2.10 <sup>ab</sup> ±0.14	1.21 <sup>ab</sup> ±0.31	65.91 <sup>b</sup> ±2.99	30.57 <sup>b</sup> ±2.6	3.53 <sup>a</sup> ±0.44
24.78 <sup>bc</sup> ±1.76	2.36 <sup>ab</sup> ±0.21	2.15 <sup>ab</sup> ±0.42	1.08 <sup>abc</sup> ±0.33	66.59 <sup>b</sup> ±1.68	7	3.17 <sup>abc</sup> ±0.26	
27.14 <sup>abc</sup> ±1.99	2.00 <sup>ab</sup> ±0.07	2.17 <sup>ab</sup> ±0.18	0.91 <sup>abc</sup> ±0.40	69.08 <sup>ab</sup> ±5.37	30.12 <sup>b</sup> ±1.4	3.27 <sup>abc</sup> ±0.31	
26.34 <sup>abc</sup> ±0.34	1.94 <sup>ab</sup> ±0.28	1.87 <sup>b</sup> ±0.47	1.35 <sup>a</sup> ±0.32	64.06 <sup>b</sup> ±2.92	9	3.50 <sup>ab</sup> ±0.62	
20.29 – 34.58	2.49 <sup>a</sup> ±0.42		1.15 <sup>abc</sup> ±0.20	66.35 <sup>b</sup> ±0.13	28.17 <sup>ab</sup> ±4.	3.16 <sup>abc</sup> ±0.13	
	1.18 – 2.83		0.54 <sup>bc</sup> ±0.38	72.77 <sup>a</sup> ±2.94	82	2.71 <sup>bc</sup> ±0.45	
			0.70 <sup>abc</sup> ±0.30	68.86 <sup>ab</sup> ±2.37	32.38 <sup>b</sup> ±2.4	2.64 <sup>c</sup> ±0.34	
			0.79 <sup>abc</sup> ±0.56	66.61 <sup>b</sup> ±3.06	5	2.65 <sup>c</sup> ±0.28	
			0.52 <sup>c</sup> ±0.19	67.71 <sup>ab</sup> ±0.82	30.50 <sup>b</sup> ±0.0	3.01 <sup>abc</sup> ±0.52	
			0.00 – 1.77	59.24 – 76.15	0	2.20 – 4.17	
					24.53 <sup>b</sup> ±2.7		
					4		
					27.60 <sup>ab</sup> ±1.		
					47		
					30.74 <sup>b</sup> ±2.9		
					4		
					29.28 <sup>ab</sup> ±1.		
					30		
					21.29 –		
					36.59		

348 In Table 2, Polar coordinates chroma ( $C_{ab}^*$ ) and hue ( $h_{ab}$ ) are shown instead of the Cartesian  
349 coordinates  $a^*$  and  $b^*$ , as they explain color better from a psychophysical point of view.  
350 Chroma in cheeses is almost entirely due to the influence of the  $b^*$  component. In addition,  
351 indicating the hue value ( $h_{ab}$ ) alone shows whether the cheese has a more yellowish or more  
352 orange appearance without the need to evaluate  $a^*$  and  $b^*$  simultaneously. Finally, the  
353 yellowness index (YI), which depends on  $b^*$  and  $L^*$ , has been shown as a common indicator  
354 of cheese color in scientific literature. Brazilian artisanal cheeses showed significant  
355 differences ( $p < 0.05$ ) for the instrumental color parameters: lightness (60.9 – 94.7), chroma  
356 (17.0 – 38.5), hue (77.2 – 109.5) and yellowness index (26.1 – 82.4). Standard deviation  
357 values showed that there is also a large variation in color parameters for the same type of  
358 cheese, which may be related to differences in the production process and storage conditions.  
359 The yellow color of the cheese ( $h_{ab} \sim 90$ ) is mainly due to the presence of carotenoids, such as  
360  $\beta$ -carotene ( $C_{40}H_{56}$ ), lutein ( $C_{40}H_{56}O_2$ ) and  $\beta$ -cryptoxanthin ( $C_{40}H_{56}O$ ) (Gentili et al., 2013). In  
361 this study, a relationship was observed between the brightness and the productive aspects of  
362 the cheeses, where the unripened cheeses (CO and MF) were characterized by lighter colors  
363 (higher values of lightness), the ripened cheeses by intermediate colors and the melted by  
364 darker colorations (lower lightness values). Regarding the yellowness index, which takes into  
365 account the color parameter  $b^*$  and brightness, it was observed that BC is more yellow, while  
366 MF and AR cheeses are more whitish.

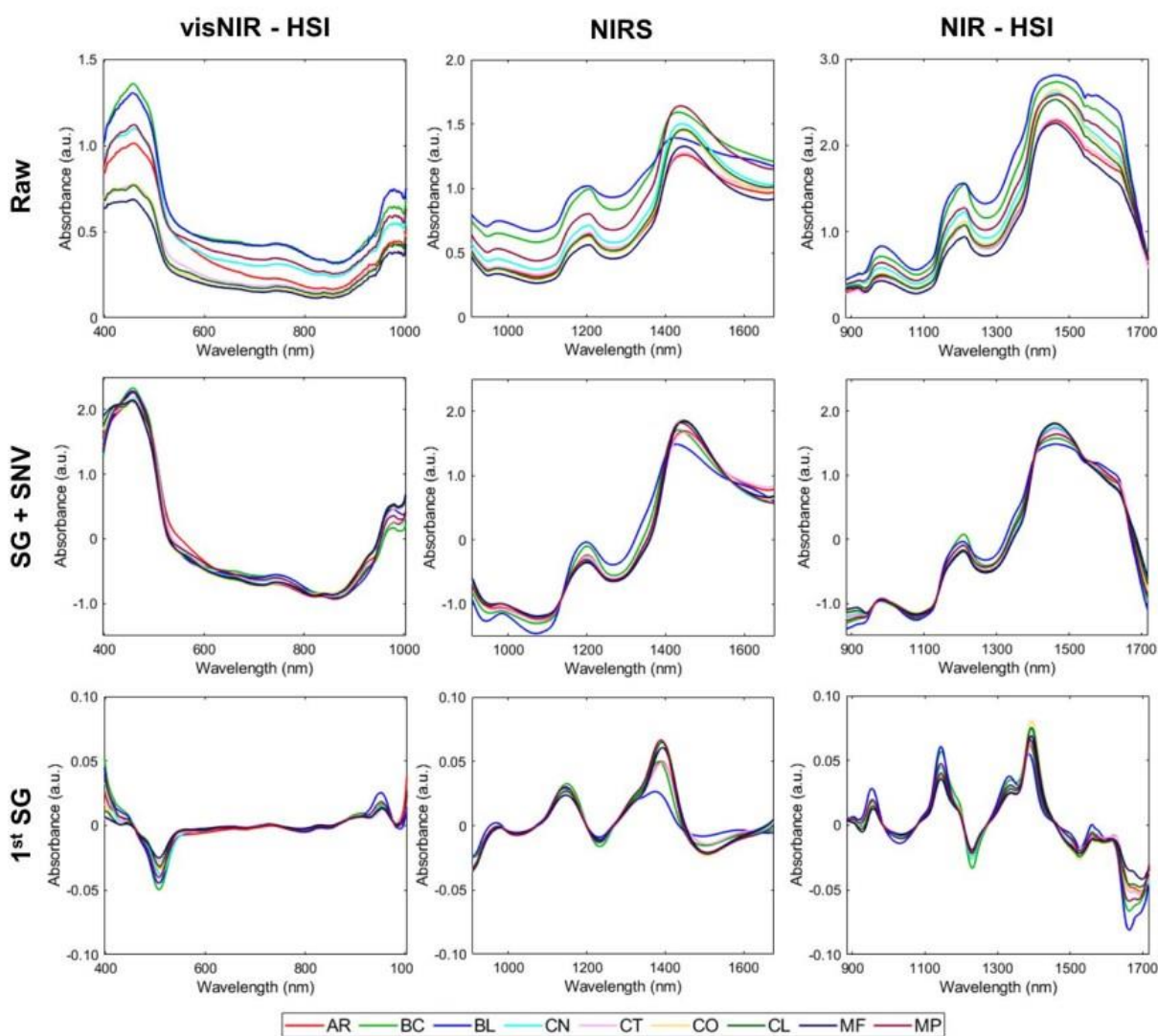
367 Table 3 presents the results of the fatty acid profile of traditional Brazilian cheeses, where  
368 statistically significant differences are observed ( $p < 0.05$ ). In general, the samples consist  
369 mainly of saturated fatty acids (SFAs) (59.24 – 76.15%), with emphasis on myristic acid  
370 ( $C_{14:0}$ , 8.36 – 13.15%), palmitic acid ( $C_{16:0}$ , 27.05 – 38.30%) and stearic ( $C_{18:0}$ , 8.32 –  
371 16.66%), followed by monounsaturated fatty acids (MUFAs) (21.29 – 36.59%), especially  
372 oleic ( $C_{18:1}$ , 20.29 – 34.58%). It is possible to observe that cheeses produced in the Northeast

373 region (CO, CL, BC, BL and MF) have a different fatty acid profile than cheeses from the  
374 South and Southeast regions (AR, CT, MP and CN), as they have lower percentages of SFAs  
375 and higher levels of PUFAs. The fatty acid profile of cheeses is directly related to the  
376 composition of milk fat (rearing system, animal feeding and time of year), as well as cheese  
377 processing, especially microbiota and maturation period (Jesus et al., 2023; 2021). Thus, these  
378 compositional differences associated with the production process and producing region can be  
379 investigated to certify the origin of the cheeses.

380

### 381 **3.2. Spectral profile**

382 The mean absorbance spectra of Brazilian traditional cheeses (Fig. 2) are comparable to those  
383 previously reported for other cheese types (Malegori et al., 2021; Reis et al., 2022; Medeiros  
384 et al., 2023). It is possible to observe different absorption bands in the visible (450 nm) and  
385 near infrared (970, 1150, 1210, 1230, 1390, 1450, 1500, 1526 and 1660-1690 nm) regions of  
386 the pre-processed spectra related to the main organic compounds present in cheese.



387

388 **Fig. 2.** vis/NIR and NIR spectra of Brazilian traditional cheeses raw, preprocessed with  
 389 Savitzky-Golay smoothing combined with SNV (SG + SNV) and with the first derivative of  
 390 Savitzky-Golay (1<sup>st</sup> SG).  
 391

392 The absorption peak at 450 nm can be attributed to the presence of carotenoids responsible for  
 393 the yellow color of cheeses (Britton et al., 2004), such as  $\beta$ -carotene, lutein and  $\beta$ -  
 394 cryptoxanthin, and/or the presence of riboflavin (vitamin B2) (Becker et al., 2003). The  
 395 absorption bands at 970 and 1450 nm correspond to second and O–H stretching in the first  
 396 overtone, characteristic of water. The absorption bands at 740, 1150, 1230, 1340-1390 and  
 397 1690 nm correspond to C–H stretching at the fourth, second and first overtone (–CH, –CH<sub>2</sub>, –  
 398 CH<sub>3</sub>), present in CH<sub>2</sub> groups in the acid chain fatty acids and their terminal CH<sub>3</sub> groups, as

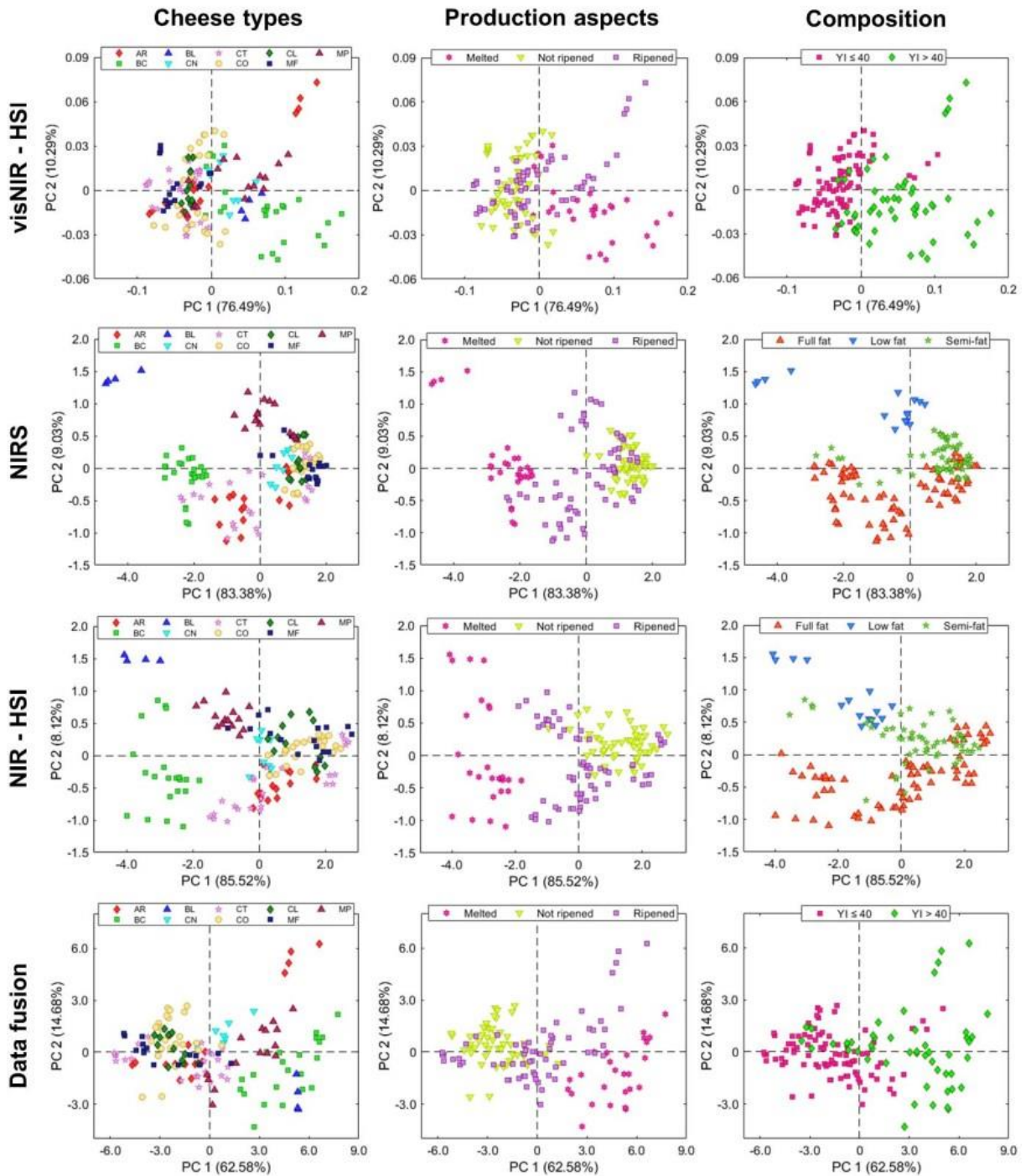
399 well as CH and CH<sub>2</sub> present in the glycerol fraction. The absorption bands at 1170 and 1660  
400 nm are attributed to C–H vibrations in the second and first overtone and are associated with  
401 the presence of unsaturated fatty acids (–HC=CH–) in the aliphatic chains of fat, especially  
402 oleic acid (C18 :1) (Osborne et al., 1993). The peaks at 910 and 1210 nm, attributed to C–H  
403 vibrations at the third and first overtone, and at 1500 and 1530 nm, attributed to N–H  
404 vibrations at the first overtone, are associated with protein content, such as casein (Frank &  
405 Birth, 1982; Osborne et al., 1993).

406

### 407 **3.3. Principal Components Analysis (PCA)**

408 Principal Component Analysis (PCA) (Fig. 3) was applied to NIRS and HSI spectra (vis/NIR,  
409 NIR and data fusion) to explore spectral variations among Brazilian traditional cheeses. The  
410 results are shown according to three groupings: cheese type, production steps (ripening and  
411 curd melting) and composition. The influence of curd heating was also investigated, but it was  
412 not observed sample separation regarding this feature.

413 The two-dimensional representation (PC1 × PC2) of the PCA scores showed that the NIR-  
414 HSI spectra explained a higher percentage of cheese variability (93.64%), followed by NIRS  
415 data (92.41%), vis/NIR-HSI (86.78 %) and the fusion of HSI spectroscopic data (77.26%).  
416 Although there is a difference in the variability explained by the first two components (PC1  
417 and PC2), the PCAs performed with the different data allow the visualization of the separation  
418 of some cheese types, especially butter cheese (BC) and Minas Padrão light cheese (MP). The  
419 overlapping of the other cheeses implies that there are other factors, in addition to the type of  
420 cheese, that influence the spectral variability of the cheeses and, consequently, the separation  
421 of the samples.



423

424 **Fig. 3.** PCA score plot of Brazilian traditional cheeses according to type, production (ripening  
 425 and curd heating), and compositional aspects (fat content and yellowness index).  
 426

427 In the PCA performed with the vis/NIR-HSI spectral data (397- 1004 nm, 1<sup>st</sup> SG) (Fig. 3) it is

428 possible to observe that the spectral variability represented by the scores of first principal

429 component was influenced to a greater extent by the color of the samples, where cheeses with  
430 lower yellowness index ( $YI \leq 40$ ) were characterized by negative scores on PC1 and the  
431 highest yellowness index ( $YI > 40$ ) by positive scores. This result is in line with the loadings  
432 plot (Fig. S2a), where it is possible to observe that variations in PC1, as well as in PC2, are  
433 associated with the content of carotenoids and/or riboflavin (440 nm) (Britton et al., 2004).  
434 The compositional aspects of the cheeses, especially the fat content, influenced the separation  
435 of samples in PC3 scores (Fig. S1 in supplementary material), where cheeses with lower fat  
436 content were characterized by negative scores and higher fat cheeses by positive scores. The  
437 biggest contributors to the separation in this main component (Fig. S2a in supplementary  
438 material) are associated with the content of carotenoids and riboflavin (430, 500 and 530 nm)  
439 (Britton et al., 2004; Becker et al., 2003) and the fat content (940 nm) (Osborne et al, 1993).  
440 In PCA models performed with NIRS (1100 – 1600 nm, SNV + 2<sup>nd</sup> SG) and NIR-HSI data  
441 (1100 – 1600 nm, SNV + 1<sup>st</sup> SG) (Fig. 3) the first principal component (PC1) is associated  
442 with changes in protein structure (especially casein) due to cheese processing. In non-ripened  
443 cheeses (CO, CL and MF), located in the positive region of PC1 scores, the enzymatic action  
444 of industrial rennet promotes limited proteolysis of k-casein (cleavage of the Phe<sub>105</sub>-Met<sub>106</sub>  
445 peptide bond) separating it into two macropeptides (Herbert et al., 1999). In ripened cheeses  
446 (AR, CT, MP and CN), distributed mainly between the negative and intermediate scores  
447 regions, in addition to enzymatic coagulation, changes occur during ripening that break  
448 cheese proteins into oligopeptides, which can additionally be degraded into shorter peptides  
449 and amino acids (Boran et al. 2023). In melted cheeses (BC and BL), spread in the negative  
450 part of PC1 scores, the main aspects of production are acid coagulation promoted by the  
451 natural microbiota of milk and the melting stage. The latter has a greater impact on the  
452 structure of the proteins, since melting salts (citrates, polyphosphates, or sodium bicarbonate)  
453 are used that promote the peptization of casein, separating its large hydrophobic aggregates



454 into smaller units (Garcia et al., 2023). Thus, it is possible to infer that the extent of changes  
455 in protein structure increases in the negative sense of PC1 scores (not ripened < ripened <  
456 melted). This behavior was also observed by Herbert et al. (1999) when studying the  
457 influence of milk coagulation types (acid, enzymatic and mixed) on tryptophan emission  
458 fluorescence spectral data, where the first principal component separated the samples  
459 according to modifications in the micellar structure. The second principal component  
460 describes the variability associated with the fat content, where it is possible to separate the  
461 samples with the highest (full fat) and lowest (low fat) content in the negative and positive  
462 part of PC2 scores, respectively. The wavelengths (Fig. S2b and S2c in supplementary  
463 material) that contributed to the separation of the samples towards PC1 and PC2 scores are  
464 associated with moisture content (1450 nm), fat (1140, 1170, 1210, 1320, 1390 and 1410 nm)  
465 and proteins (1190 and 1510 nm) (Osborne et al., 1993)

466 From an exploratory point of view, the fusion of HSI spectroscopic data (vis/NIR + NIR) (397  
467 – 1600 nm, SNV + 1<sup>st</sup> SG) did not promote sample separation beyond what was observed for  
468 the separate techniques. In the first principal component (PC1) scores it is possible to observe  
469 a trend of sample separation according to the structural modifications of the proteins, as  
470 observed in the PCA performed with the NIR data, while the influence of the yellowness  
471 index is also observed, like the observed in the PCA for the vis/NIR data. In the loadings of  
472 PCA applied to the data fused (Fig. S3d in supplementary material) it is possible to observe  
473 that the wavelengths that influenced the separation in PC1 and PC2 scores are the same ones  
474 reported in vis/NIR-HSI and NIR-HSI separately, which are associated with the carotenoid  
475 content (490 nm), water (970 nm), fat (1140, 1230, 1330 and 1410 nm) and proteins  
476 (1500nm) (Osborne et al., 1993).

477

#### 478 **3.4. Classification models**

479

480 PLS-DA classification models (Table 4) based on spectral information (NIR, vis/NIR-HSI,  
481 NIR-HSI and HSI data fusion) were constructed to discriminate traditional Brazilian cheeses.  
482 The performances of these models were compared with the model based on chemical  
483 composition data to investigate the potential of spectroscopy as a tool to assist in the  
484 certification of these products. The chemical composition parameters used in the construction  
485 of the model were the fatty acids C6:0, C8:0, C10:0, C12:0, C14:0, C18:0, C18:1, C18:3,  
486 SFAs and MUFAs), as they provided better prediction results.

487 It is possible to observe that the models performed with spectral information presented better  
488 classification performances, with higher sensitivity ( $\geq 0.75$ ) and specificity ( $\geq 0.84$ ) values  
489 and lower error rates (11 - 18%), compared to the model built only with chemical composition  
490 information (33% error rate). This result is justified by the large amount of information  
491 contained in the spectra, which is influenced by the composition and productive aspects, as  
492 observed in the PCA. Comparing the results of the three devices, the best classification index  
493 was obtained using information in the near infrared region (NIRS), where the sensitivity and  
494 specificity values were 0.95 and 0.84, respectively, and the classification rate 89% correct.  
495 Fusion of HSI spectroscopic data did not improve cheese discrimination (84% accuracy).

496

497 **Table 4.** Figures of merit of PLSDA models to classify Brazilian traditional cheese types.

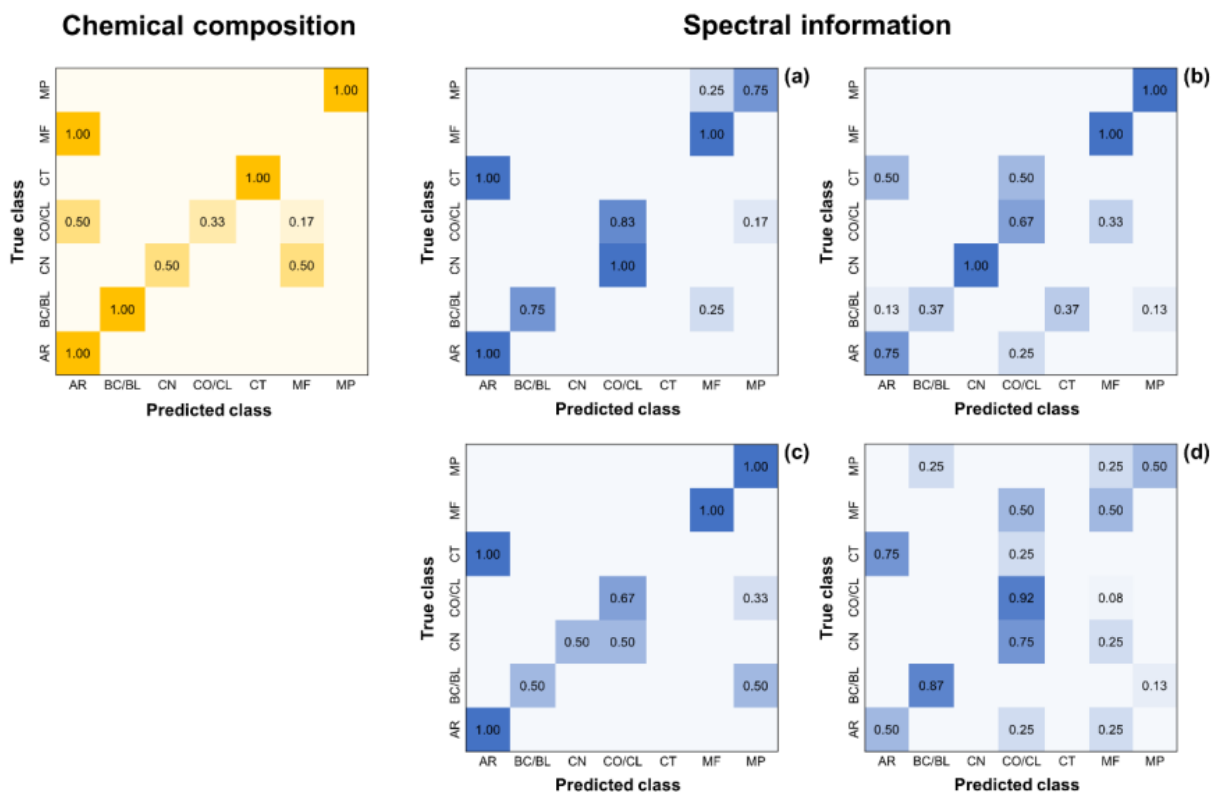
Equipment	Pre-processing	Variables	LV	Calibration			Prediction		
				Sens	Spec	Acc	Sens	Spec	Acc
Chemical composition	Autoscale	Fatty acids*	3	0.85	0.76	0.81	0.57	0.76	0.67
vis/NIR-HSI	2 <sup>nd</sup> + SNV	iPLS	5	0.94	0.93	0.82	0.75	0.89	0.82
NIRS	1 <sup>st</sup> SG	1050 - 1350, 1600 - 1680nm	5	0.96	0.90	0.93	0.95	0.84	0.89
NIR-HSI	1 <sup>st</sup> SG	iPLS	4	0.94	0.88	0.91	0.85	0.85	0.85
Data fusion	1 <sup>st</sup> SG	780 - 1600 nm	6	0.88	0.89	0.89	0.81	0.87	0.84

498

\*C6:0, C8:0, C10:0, C12:0, C14:0, C18:0, C18:1, C18:3, SFAs e MUFAs.



499 The distribution of validation samples into classes (Fig. 4) showed that the largest  
 500 classification errors in the model based on chemical composition, the largest errors were  
 501 observed for CO/CL and MF cheeses, which were incorrectly classified as AR cheese. In  
 502 models based on spectral information, the largest errors were observed for samples of CT and  
 503 for coalho cheeses (CO/CL), where samples of CT cheese were identified as AR or coalho  
 504 cheese (CO/CL), and coalho samples (CO/CL) were incorrectly classified as MF or MP. The  
 505 wavelengths that contributed to the classification of cheeses in the visible region are related to  
 506 the lipid fraction (930 nm), carotenoids (450 nm) and water (970 nm). In the infrared region,  
 507 the wavelengths with the greatest contribution are centered in spectral regions associated with  
 508 the content of water (970 3 1440 nm), fat (930, 1150, 1220 and 1275 nm) and proteins (1540  
 509 nm).  
 510



511

512 **Fig. 4.** Confusion matrix (external validation) of PLS-DA models based on chemical  
 513 composition data and spectral information: vis/NIR-HIS (a), NIRS (b), NIR-HIS (c) and HSI  
 514 spectroscopic dataset fusion (d).

515

### 516 **3.5. Prediction models**

517 PLS regression models were developed to compare the performance of three spectrometers  
 518 (NIR, vis/NIR-HSI and NIR-HSI) and fusion spectroscopic data (vis/NIR-HSI and NIR-HSI)  
 519 in predicting moisture, fat, protein and ash in Brazilian traditional cheeses. The influence of  
 520 pre-processing and spectral region on the statistical parameters of the models was  
 521 investigated, so that the best results are presented in Table 5. Figures of merit for the ash  
 522 models are not reported here because they did not performed values sufficiently relevant  
 523 regarding model performance.

524 In our study it was observed that only the model developed to predict protein content using  
 525 the NIRS spectrum presented better results with the raw spectrum (without pre-processing).  
 526 Even in this case, the best result was obtained by reducing the spectrum from 908 - 1676 nm  
 527 to 1100 -1660 nm. Thus, in general, the models performed with pre-processed spectra and/or  
 528 with the selection of wavelengths related to the target chemical attribute showed superior  
 529 predictive performance than those using the raw data (full spectrum without pre-processing).  
 530 When the calibration and cross-validation results of the models obtained for the different  
 531 instruments were compared, the fusion of the spectral data showed slightly better results.  
 532 However, the performance of the devices to predict in the external set varied according to the  
 533 chemical components.

534

535 **Table 5.** Figures of merit of PLSR models to predict moisture, fat, and protein content in  
 536 Brazilian traditional cheeses.

Equipment	Pre-processing	Spectral range	LV	Calibration		Cross-validation		Prediction		
				$R_C^2$	RMSEC	$R_{CV}^2$	RMSECV	$R_p^2$	RMSEP	RPD
<i>Moisture</i>										
vis/NIR-HSI	SNV + 1 <sup>st</sup> SG	780 - 1000 nm	4	0.88	1.65	0.86	1.79	0.84	1.34	2.54

NIRS	1 <sup>st</sup> SG	iPLS	5	0.87	1.70	0.86	1.73	0.85	1.36	2.51
NIR-HSI	SNV + 1 <sup>st</sup> SG	iPLS	5	0.89	1.54	0.88	1.66	0.90	1.32	2.59
Dafa fusion	SNV + 1 <sup>st</sup> SG	397 - 1717 nm	5	0.91	1.38	0.88	1.62	0.90	1.27	2.69
<b><i>Fat</i></b>										
vis/NIR-HSI	1 <sup>st</sup> SG	397 - 1007 nm	4	0.87	2.28	0.83	2.58	0.84	2.17	2.49
NIRS	SNV + 2 <sup>nd</sup> SG	1100 - 1600 nm	5	0.88	2.14	0.85	2.39	0.85	2.17	2.49
NIR-HSI	SG + SNV	1050 - 1350, 1600 - 1680 nm	7	0.87	2.29	0.83	2.56	0.82	2.52	2.08
Dafa fusion	1 <sup>st</sup> SG	397 - 1600 nm	6	0.90	1.98	0.87	2.24	0.81	2.33	2.25
<b><i>Protein</i></b>										
vis/NIR-HSI	SNV + 1 <sup>st</sup> SG	iPLS	5	0.73	1.10	0.69	1.16	0.57	0.99	1.50
NIRS	Raw	1100 - 1600 nm	6	0.80	0.94	0.72	1.12	0.73	1.01	1.47
NIR-HSI	SNV + 1 <sup>st</sup> SG	iPLS	5	0.83	0.88	0.79	0.97	0.78	0.93	1.58
Dafa fusion	SNV + 1 <sup>st</sup> SG	397 - 1717 nm	5	0.84	0.81	0.78	0.95	0.67	0.91	1.62

537

538 The best model to predict the moisture content was obtained from the fusion of the HSI  
539 spectroscopic data set (vis/NIR + NIR), where an  $R_p^2$  of 0.90 and RMSEP of 1.27% were  
540 obtained. The variables that most contributed to this performance are centered around 508,  
541 1120, 1140, 1170, 1225, 1320, 1395, 1510, 1560 and 1660 nm and are associated with the  
542 content of other chemical components present in the cheese, such as fat, proteins, and  
543 carotenoids (Britton et al., 2004; Osborne et al., 1993). Although the visible region has  
544 contributed to this result, it is possible to obtain similar results for the prediction of moisture  
545 content from the other equipment ( $R_p^2$  between 0.84 and 0.90 and RMSEP close to 1.3) using  
546 only the near infrared region. According to the RPD values, all models can be applied to  
547 predict the moisture content with good performance (RPD between 2.5 and 3.0).

548 The best models to predict fat content were obtained with NIRS and vis/NIR-HSI spectra,  
549 where  $R_p^2 \sim 0.85$  and RMSEP of 2.17% were observed. The variables that contributed to the  
550 performance of the NIRS model are mainly associated with the CH, CH<sub>2</sub> and CH<sub>3</sub> groups  
551 present in the aliphatic chains of fat (1170, 1215, 1360, 1395, 1415 nm) and, to a lesser  
552 extent, with structures present in proteins (1430 nm) and water (1450 nm). In the vis/NIR  
553 model, a strong contribution of wavelengths associated with fat content (950 nm) was also  
554 observed. However, it is interesting to emphasize that the greatest contribution was observed  
555 in the visible spectrum (430 and 505 nm), which is associated with carotenoid content. This



556 result is expected, because in addition to carotenoids contributing to the yellowish color of  
557 cheeses, they are solubilized in the fat fraction. Similarly, Stocco et al. (2019) observed that  
558 models built with the vis/NIR region (350 – 1830 nm) presented similar performances to  
559 those based on the NIR region (1100 – 1830 nm) ( $R_p^2$  of 0.85 and RPD of 2.03), when  
560 comparing the performance of two spectrometers and spectrum intervals to predict the fat  
561 content in cheeses. All models predicting fat content showed RPD between 2.0 and 2.5,  
562 indicating that they can be used for screening purposes.

563 The fusion of the HSI spectroscopic dataset (vis/NIR + NIR) showed the best result for  
564 predicting protein content, with calibration and prediction errors close to 0.9%. The  
565 wavelengths that contributed to the performance of the model are associated with protein  
566 content (1510 nm) and structures associated with carotenoids (508 nm) and fat (1145, 1225,  
567 1395 and 1660 nm). It is possible to predict the protein content without loss of performance  
568 ( $R_p^2$  of 0.78 and error of 0.93%) using the NIR-HSI spectra and to obtain approximate results  
569 using the other equipment (between 0.57 and 0.73 and errors of ~1.0%). However, according  
570 to the RPD values, only models based on the fusion of spectroscopic data and NIR-HSI are  
571 indicated for estimating the protein content, as they are able to distinguish between high and  
572 low levels of this compound ( $1.5 < \text{RPD} < 2.0$ ).

573 Few studies available in the scientific literature have investigated the use of different  
574 spectrometers and spectral ranges in the vis and NIR ranges to predict chemical characteristics  
575 of a wide type of cheeses. This number is even lower when looking for studies that developed  
576 models from spectra acquired with whole cheese (without any sampling, grinding or other  
577 preparation). The discussion, therefore, focuses mainly on studies that used this last criterion  
578 and was carried out in terms of RMSEP and RPD, since the coefficient of determination ( $R^2$ )  
579 is influenced by the range of reference values.



580 Wiedemair et al (2019) compared the performance of models based on vis/NIR (740 – 1070  
581 nm) and NIR (800 – 2500 nm) spectra to predict the composition of hard and semi-hard  
582 cheeses (n = 46). These authors reported results in accordance to this current work and  
583 observed better performance for moisture prediction using the NIR spectrum (RMSEP of 1.10  
584 and RPD of 5.60). On the other hand, fat content was predicted with lower error (RMSEP of  
585 1.19 and RPD of 7.75) from vis/NIR spectra. Stocco et al. (2019) developed PLS models to  
586 predict compositional characteristics of a wide type of cheeses (197 samples from 37  
587 categories) using a portable vis/NIR spectrometer (350 - 1830 nm) and obtained performance  
588 (RMSEP) very close to those reported in this study to predict fat ( 2.03%, 350 - 1830 nm) and  
589 proteins (1.57%, 850 - 1050 nm), and slightly lower for moisture prediction (2.00%, 1100 -  
590 1830 nm). Ayvaz et al (2021) when predicting the composition of Ezine cheese from different  
591 species (n = 81) using an FTIR spectrophotometer (10000 – 4000 cm<sup>-1</sup>) obtained superior  
592 results for moisture (RPD of 3.38) and similar results for fat (RPD of 2.14) and proteins (RPD  
593 of 1.47).

594 The results obtained in this study were lower than those reported for predicting fat content in  
595 Emmental cheese (n = 91, RMSEP of 0.39% and RPD of 3.82) (Karoui et al., 2006), Grana  
596 Padano (n = 190, RMSEP of 1.19%) (Marinoni et al., 2017) and ricotta (n = 19, RMSECV of  
597 1.9%) (Madalozzo et al., 2015). The smaller errors obtained in these studies are justified by  
598 the high homogeneity of the sample set, since only one category of cheese was included. The  
599 results are also lower than those obtained for models based on spectra acquired with  
600 crushed/grated cheese. This result is expected, as predicting cheese composition from the  
601 outer surface spectrum is more challenging. Although grinding produces better performances  
602 (Ayvaz et al., 2021; Wiedemair et al., 2019; Marinoni et al., 2017), it confronts the non-  
603 destructive character of vis/NIR spectroscopy and limits its application in the rapid  
604 authentication of cheeses with of origin or protected geographical indication.

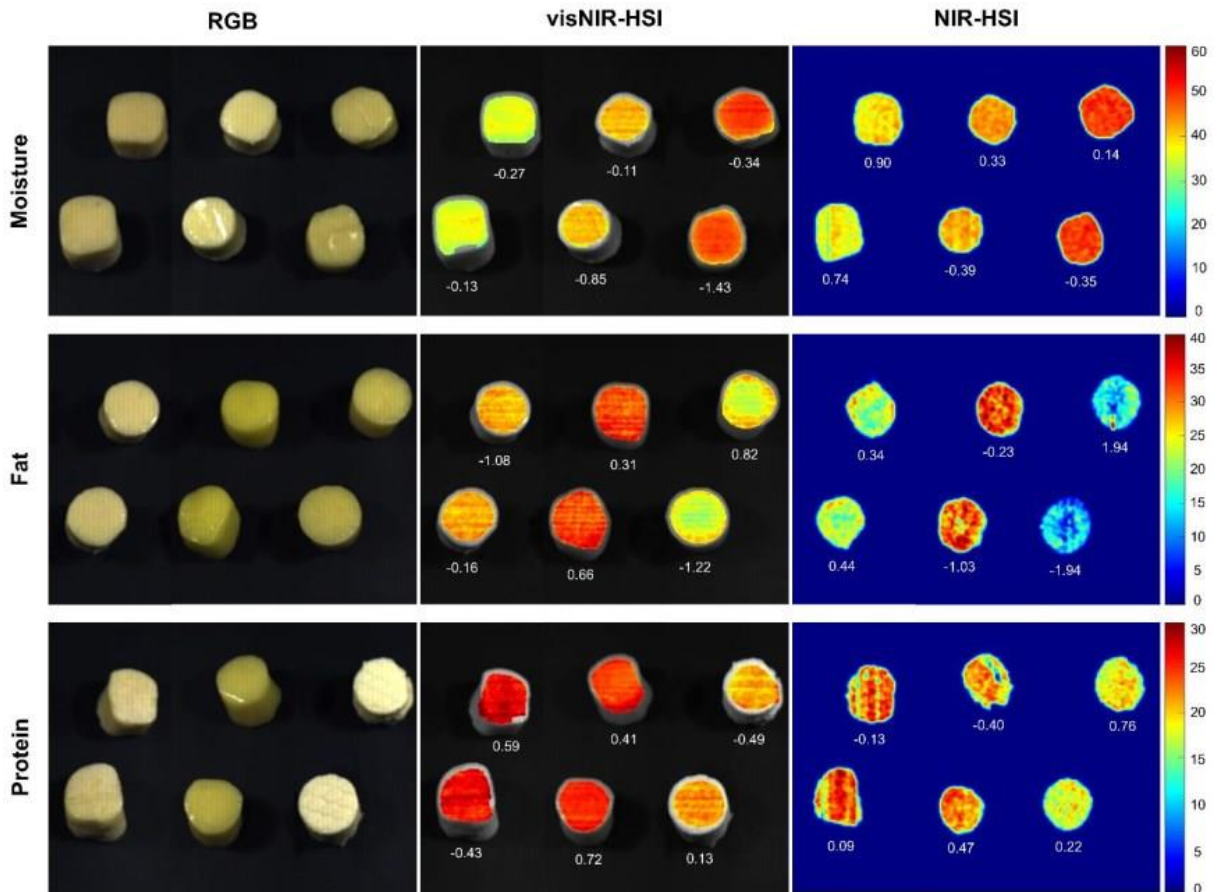
605

606 **3.6. Chemical maps of moisture, fat, and protein**

607 The best models obtained for the vis/NIR-HSI and NIR-HSI data were applied to each pixel  
608 from ROI of the images to visualize the distribution of moisture, fat, and protein in the cheese  
609 samples, obtaining a pseudo-color image, or chemical map. Fig. 5 shows some maps of the  
610 spatial distribution of the predicted chemical properties in different types of cheese. The  
611 values presented in the lower corner of each cheese cylinder correspond to the absolute error  
612 (%), calculated by subtracting the reference value and that predicted by the model.

613 One of the greatest advantages of using hyperspectral imaging, compared to RGB imaging  
614 and conventional spectroscopy, is that it is possible to observe the concentration distribution  
615 of the modeled analyte. In the RGB image (Fig. 5) one can observe differences in the color  
616 and texture of the external surface of the samples due to the presence of different types of  
617 cheese, while the compositional differences are practically imperceptible. On the other hand,  
618 hyperspectral imaging allows you to clearly visualize differences in composition by the color  
619 intensity of each pixel in the chemical map.

620 Comparing the spatial distribution maps vis/NIR-HSI and NIR-HSI it is possible to observe a  
621 difference in the homogeneity and color intensity of the pixels for the same sample. This  
622 observation may be related to the difference in resolution between the images and the  
623 heterogeneous distribution of analytes in the sample. Despite this, there are no major  
624 differences between the results obtained by the reference method and those predicted by the  
625 two devices.



626  
627  
628

**Fig. 5.** RGB images and spatial distribution maps of moisture, fat and protein content based on vis/NIR-HSI and NIR-HSI data.



629

630 It is important to mention that the vis/NIR-HSI and NIR-HSI models (based on the spectra  
631 acquired on the external surface) presented a low average error to predict the composition of  
632 the samples from the images of the internal part of the cheese, with average absolute errors of  
633 0.32 and 0.00% for moisture, 1.01 and 0.31% for fat, and 0.33 and 0.06% for protein,  
634 respectively. These results indicate that, even though some cheeses have composition  
635 gradients due to proteolytic, lipolytic and dehydration phenomena that occur during  
636 maturation, the information obtained from the external surface is sufficient to predict its  
637 composition satisfactory accuracy. Hence, these models can be used to predict the  
638 composition of Brazilian cheeses used in this study and also enhanced including additional  
639 types of cheese and can be useful to study compositional changes that occur during  
640 maturation.

641

#### 642 **4. Conclusion**

643 This study compared the feasibility of hyperspectral imaging (vis/NIR-HSI, NIR-HSI and  
644 data fusion) and conventional (NIRS) spectrometers to characterize Brazilian traditional  
645 cheeses. Principal component analysis (PCA) showed that the spectral variability of Brazilian  
646 traditional cheeses in the vis/NIR is related to differences in color and fat content, while in the  
647 NIR there is a greater influence of productive aspects and fat content.

648 The PLS-DA models showed that the spectrum in the near infrared region (NIRS) has  
649 relevant information to discriminate the types of Brazilian artisanal cheeses, indicating that  
650 this technique can be used as a useful tool in investigating the authenticity of cheeses  
651 according to the region of origin.

652 The PLS models demonstrated that it is possible to efficiently predict the chemical  
653 composition (moisture, fat, and protein) of a wide type of cheeses. Hyperspectral imaging

654 equipment (vis/NIR-HSI and NIR-HSI) can be recommended, especially when there is great  
655 heterogeneity within the sample and/or when there is interest in studying and visualizing  
656 compositional changes, as the general quantitative results obtained are comparable to the  
657 technique punctual (NIRS). The latter, in turn, is more attractive from an economic and  
658 operational point of view, due to lower cost, portability and shorter processing time. Finally,  
659 and in this case, the fusion of HSI spectroscopic data (vis/NIR + NIR) did not provide  
660 significant improvement of the predictive capability to justify its recommendation, because  
661 despite providing better performances to predict moisture and proteins, these are not  
662 substantially greater to justify its use.

663

#### 664 **Declaration of Competing Interest**

665 The authors declare that they have no known competing financial interests or personal  
666 relationships that could have appeared to influence the work reported in this paper.

667

#### 668 **Acknowledgments**

669 This study was financed in part by the Coordenação de Aperfeiçoamento de Pessoal de Nível  
670 Superior - Brasil (CAPES) - Finance Code 001. Maria Lucimar da Silva Medeiros  
671 acknowledges scholarship funding from CNPq (300145/2022-5) and Santander international  
672 mobility program for graduate students. Prof. Douglas Fernandes Barbin is CNPq research  
673 fellow (308260/2021-0).

674

#### 675 **References**

676 Andrade, B. M., Margalho, L. P., Batista, D. B., Lucena, I. O., Kamimura, B. A., Balthazar,  
677 C. F., Brexó, R. P., Pia, A. K. R., Costa, R. A. S., Cruz, A. G., Granato, D., Sant'Ana,  
678 A. S., Luna, A. S., & de Gois, J. S. (2022). Chemometric classification of Brazilian  
679 artisanal cheeses from different regions according to major and trace elements by ICP-

680 OES. *Journal of Food Composition and Analysis*, 109, 104519.  
681 <https://doi.org/10.1016/j.jfca.2022.104519>

682 Amigo, J. M. (2019). *Hyperspectral and multispectral imaging: setting the scene* (pp. 3–16).  
683 <https://doi.org/10.1016/B978-0-444-63977-6.00001-8>

684 AOAC. (2012). *Official Methods of Analysis* (19th ed.). AOAC Internacional.

685 Ayvaz, H., Mortas, M., Dogan, M. A., Atan, M., Yildiz Tiryaki, G., & Karagul Yuceer, Y.  
686 (2021). Near- and mid-infrared determination of some quality parameters of cheese  
687 manufactured from the mixture of different milk species. *Journal of Food Science and*  
688 *Technology*, 58(10), 3981–3992. <https://doi.org/10.1007/s13197-020-04861-0>

689 Becker, E. M., Christensen, J., Frederiksen, C. S., & Haugaard, V. K. (2003). Front-Face  
690 Fluorescence Spectroscopy and Chemometrics in Analysis of Yogurt: Rapid Analysis of  
691 Riboflavin. *Journal of Dairy Science*, 86(8), 2508–2515.  
692 [https://doi.org/10.3168/jds.S0022-0302\(03\)73845-4](https://doi.org/10.3168/jds.S0022-0302(03)73845-4)

693 Bezerra, T. K. A., Arcanjo, N. M. O., Garcia, E. F., Gomes, A. M. P., Queiroga, R. de C. R.  
694 do E., Souza, E. L., & Madruga, M. S. (2017). Effect of supplementation with probiotic  
695 lactic acid bacteria, separately or combined, on acid and sugar production in goat  
696 ‘coalho’ cheese. *LWT*, 75, 710–718. <https://doi.org/10.1016/j.lwt.2016.10.023>

697 Boran, O. S., Sulejmani, E., & Hayaloglu, A. A. (2023). Acceleration of proteolysis, flavour  
698 development and enhanced bioactivity in a model cheese using Kuflu cheese slurry: An  
699 optimisation study. *Food Chemistry*, 412, 135495.  
700 <https://doi.org/10.1016/j.foodchem.2023.135495>

701 Brasil (1996). Regulamentos Técnicos de Identidade e Qualidade dos Produtos Lácteos.  
702 Portaria nº 146 de 07 de março de 1996, Pub. L. No. 146, Diário Oficial da União.  
703 Retrieved March 17, 2023 from:  
704 [https://www.defesa.agricultura.sp.gov.br/legislacoes/portaria-mapa-146-de-07-03-](https://www.defesa.agricultura.sp.gov.br/legislacoes/portaria-mapa-146-de-07-03-1996,669.html)  
705 [1996,669.html](https://www.defesa.agricultura.sp.gov.br/legislacoes/portaria-mapa-146-de-07-03-1996,669.html)

706 Brasil (1996). Regula direitos e obrigações relativos à propriedade industrial. Lei nº 9.279, de  
707 14 de maio de 1996, Pub. L. No. 9.279, Diário Oficial da União (1997). Retrieved  
708 february 17, 2024 from: [https://www.planalto.gov.br/ccivil\\_03/leis/19279.htm](https://www.planalto.gov.br/ccivil_03/leis/19279.htm)

709 Brasil (1997). Regulamento Técnico para Fixação de Identidade e Qualidade de Queijo Minas  
710 Frescal. Portaria nº 352 de 04 de setembro de 1997, Pub. L. No. 352, Diário Oficial da  
711 União (1997). Retrieved march 17, 2023 from:  
712 [https://sidago.agrodefesa.gov.br/site/adicionaispropios/protocolo/arquivos/409853.p](https://sidago.agrodefesa.gov.br/site/adicionaispropios/protocolo/arquivos/409853.pdf)  
713 [df](https://sidago.agrodefesa.gov.br/site/adicionaispropios/protocolo/arquivos/409853.pdf)

714 Brasil (2001). Regulamentos Técnicos de Identidade e Qualidade de Manteiga da Terra ou  
715 Manteiga de Ganafa; Queijo de Coalho e Queijo de Manteiga. Instrução Normativa nº  
716 30 de 26 de junho de 2001, Pub. L. No. 30, Diário Oficial da união. Retrieved  
717 December 08, 2022 from:  
718 [https://pesquisa.in.gov.br/imprensa/jsp/visualiza/index.jsp?data=16/07/2001&jornal=1&](https://pesquisa.in.gov.br/imprensa/jsp/visualiza/index.jsp?data=16/07/2001&jornal=1&pagina=13&totalArquivos=219)  
719 [pagina=13&totalArquivos=219](https://pesquisa.in.gov.br/imprensa/jsp/visualiza/index.jsp?data=16/07/2001&jornal=1&pagina=13&totalArquivos=219)

720 Brasil (2018). Dispõe sobre o processo de fiscalização de produtos alimentícios de origem  
721 animal produzidos de forma artesanal. Lei nº 13.680, de 14 de junho de 2018. Retrieved  
722 march 17, 2023 from: [http://www.planalto.gov.br/ccivil\\_03/\\_](http://www.planalto.gov.br/ccivil_03/_ato2015-2018/2018/lei/L13680.htm)  
723 [ato2015-](http://www.planalto.gov.br/ccivil_03/_ato2015-2018/2018/lei/L13680.htm)  
724 [2018/2018/lei/L13680.htm](http://www.planalto.gov.br/ccivil_03/_ato2015-2018/2018/lei/L13680.htm)

724 Brasil (2020). Identidade e os requisitos de qualidade que deve apresentar o produto  
725 denominado queijo minas padrão. Instrução Normativa nº 66 de 21 de julho de 2020,  
726 Pub. L. No. 66, Diário Oficial da União. Retrieved march 17, 2023 from:  
727 [https://www.in.gov.br/en/web/dou/-/instrucao-normativa-n-66-de-21-de-julho-de-2020-](https://www.in.gov.br/en/web/dou/-/instrucao-normativa-n-66-de-21-de-julho-de-2020-268265894)  
728 [268265894](https://www.in.gov.br/en/web/dou/-/instrucao-normativa-n-66-de-21-de-julho-de-2020-268265894)



- 729 Britton, G., Liaaen-Jensen, S., & Pfander, H. (2004). *Carotenoids Handbook*. Birkhuser  
730 Verlag.
- 731 CIE, C. I. de l'Éclairage. (1978). *Recommendations on uniform colour spaces, colour-*  
732 *difference equations, psychometric colour terms. Supplement No.2 to CIE 15-1971.*  
733 Bureau Central de la CIE Paris.
- 734 Costa, J. R., Pereira, D. A., de Paula, I. L., de Abreu, L. R., Pinto, S. M., Edwards, H. G. M.,  
735 Stephani, R., & de Oliveira, L. F. C. (2022). The taste of a champion: Characterization  
736 of traditional cheeses from the Minas Gerais region (Brazil) by Raman spectroscopy and  
737 microstructural analysis. *Journal of Food Composition and Analysis*, *112*, 104704.  
738 <https://doi.org/10.1016/j.jfca.2022.104704>
- 739 Fittzum, A. C., Lima, L. S., Judacewski, P., Salem, R. D. S., de Dea Lindner, J., Demiate, I.  
740 M., Zielinski, A. A. F., Alberti, A., & Nogueira, A. (2023). Evaluation of traditional  
741 semi-hard Brazilian cheeses using chemometric tools to identify possible denomination  
742 fraud. *International Journal of Dairy Technology*. [https://doi.org/10.1111/1471-](https://doi.org/10.1111/1471-0307.12954)  
743 [0307.12954](https://doi.org/10.1111/1471-0307.12954)
- 744 Francis, F. J., & Clydesdale, F. M. (1975). *Food Colorimetry: Theory and Applications*. AVI  
745 Publishing.
- 746 Frank, J. F., & Birth, G. S. (1982). Application of Near Infrared Reflectance Spectroscopy to  
747 Cheese Analysis. *Journal of Dairy Science*, *65*(7), 1110–1116.  
748 [https://doi.org/10.3168/jds.S0022-0302\(82\)82319-9](https://doi.org/10.3168/jds.S0022-0302(82)82319-9)
- 749 Garcia, A., Alting, A., & Huppertz, T. (2023). Disruption of casein micelles by calcium  
750 sequestering salts: From observations to mechanistic insights. *International Dairy*  
751 *Journal*, *142*, 105638. <https://doi.org/10.1016/j.idairyj.2023.105638>
- 752 Gentili, A., Caretti, F., Bellante, S., Ventura, S., Canepari, S., & Curini, R. (2013).  
753 Comprehensive Profiling of Carotenoids and Fat-Soluble Vitamins in Milk from  
754 Different Animal Species by LC-DAD-MS/MS Hyphenation. *Journal of Agricultural*  
755 *and Food Chemistry*, *61*(8), 1628–1639. <https://doi.org/10.1021/jf302811a>
- 756 Hayaloglu, A. A., & McSweeney, P. L. H. (2014). Primary biochemical events during cheese  
757 ripening. In *Dairy Microbiology and Biochemistry: Recent Developments*.  
758 10.1201/b17297-8.
- 759 Herbert, S., Riaublanc, A., Bouchet, B., Gallant, D. J., & Dufour, E. (1999). Fluorescence  
760 Spectroscopy Investigation of Acid-or Rennet-Induced Coagulation of Milk. *Journal of*  
761 *Dairy Science*, *82*(10), 2056–2062. [https://doi.org/10.3168/jds.S0022-0302\(99\)75446-9](https://doi.org/10.3168/jds.S0022-0302(99)75446-9)
- 762 Ibáñez, R. A., Govindasamy-Lucey, S., Jaeggi, J. J., Johnson, M. E., McSweeney, P. L. H., &  
763 Lucey, J. A. (2020). Low- and reduced-fat milled curd, direct-salted Gouda cheese:  
764 Comparison of lactose standardization of cheesemilk and whey dilution techniques.  
765 *Journal of Dairy Science*, *103*(2), 1175–1192. <https://doi.org/10.3168/jds.2019-17292>
- 766 Jesus Filho, M., Klein, B., Wagner, R., & Godoy, H. T. (2021). Key aroma compounds of  
767 Canastra cheese: HS-SPME optimization assisted by olfactometry and chemometrics.  
768 *Food Research International*, *150*, 110788.  
769 <https://doi.org/10.1016/j.foodres.2021.110788>
- 770 Jesus Filho, M., Klein, B., Quintão Teixeira, L. J., Silva, J. G. S., Pallone, J. A. L., Wagner,  
771 R., & Godoy, H. T. (2023). The influence of production units and seasons on the  
772 physicochemical characteristics, mineral and fatty acid content, and texture profile of  
773 the artisanal cheeses from Serra da Canastra, Brazil. *Journal of Food Composition and*  
774 *Analysis*, *123*, 105589. <https://doi.org/10.1016/j.jfca.2023.105589>
- 775 Karoui, R., Mouazen, A. M., Dufour, É., Pillonel, L., Schaller, E., Picque, D., de  
776 Baerdemaeker, J., & Bosset, J.-O. (2006). A comparison and joint use of NIR and MIR  
777 spectroscopic methods for the determination of some parameters in European Emmental

778 cheese. *European Food Research and Technology*, 223(1), 44–50.  
779 <https://doi.org/10.1007/s00217-005-0110-2>

780 Koutina, G., Christensen, M., Bakman, M., Andersen, U., & Skibsted, L. H. (2016). Calcium  
781 induced skim-milk gelation during heating as affected by pH. *Dairy Science &*  
782 *Technology*, 96(1), 79–93. <https://doi.org/10.1007/s13594-015-0240-7>

783 Madalozzo, E. S., Sauer, E., & Nagata, N. (2015). Determination of fat, protein and moisture  
784 in ricotta cheese by near infrared spectroscopy and multivariate calibration. *Journal of*  
785 *Food Science and Technology*, 52(3), 1649–1655. [https://doi.org/10.1007/s13197-013-](https://doi.org/10.1007/s13197-013-1147-z)  
786 [1147-z](https://doi.org/10.1007/s13197-013-1147-z)

787 Malegori, C., Oliveri, P., Mustorgi, E., Boggiani, M. A., Pastorini, G., & Casale, M. (2021).  
788 An in-depth study of cheese ripening by means of NIR hyperspectral imaging: Spatial  
789 mapping of dehydration, proteolysis and lipolysis. *Food Chemistry*, 343, 128547.  
790 <https://doi.org/10.1016/j.foodchem.2020.128547>

791 Margalho, L. P., Kamimura, B. A., Pimentel, T. C., Balthazar, C. F., Araujo, J. V. A., Silva,  
792 R., Conte-Junior, C. A., Raices, R. S. L., Cruz, A. G., & Sant’Ana, A. S. (2021). A large  
793 survey of the fatty acid profile and gross composition of Brazilian traditional cheeses.  
794 *Journal of Food Composition and Analysis*, 101, 103955.  
795 <https://doi.org/10.1016/j.jfca.2021.103955>

796 Marinoni, L., Stroppa, A., Barzaghi, S., Cremonesi, K., Pricca, N., Meucci, A., Pedrolini, G.,  
797 Galli, A., & Cabassi, G. (2019). On site monitoring of Grana Padano cheese production  
798 using portable spectrometers. In *Proceedings of the 18th International Conference on*  
799 *Near Infrared Spectroscopy* (pp. 85–90). IM Publications Open LLP.  
800 <https://doi.org/10.1255/nir2017.085>

801 Masotti, F., Cattaneo, S., Stuknyte, M., Pica, V., & De Noni, I. (2020). Analytical advances in  
802 the determination of calcium in bovine milk, dairy products and milk-based infant  
803 formulas. *Trends in Food Science & Technology*, 103, 348–360.  
804 <https://doi.org/10.1016/j.tifs.2020.07.013>

805 Medeiros, M. L. da S., Lima, A. F., Gonçalves, M. C., Godoy, H. T., & Barbin, D. F. (2023).  
806 Portable near-infrared (NIR) spectrometer and chemometrics for rapid identification of  
807 butter cheese adulteration. *Food Chemistry*, 136461.  
808 <https://doi.org/10.1016/j.foodchem.2023.136461>

809 Minas Gerais (2008). Regulamenta o processo de produção de Queijo Minas Artesanal.  
810 Decreto nº 44.864 de 01 de agosto de 2008, Pub. L. No. 44.864, Diário Oficial do  
811 Estado de Minas Gerais. Retrieved march 17, 2023 from:  
812 [https://cdn.sertaobras.org.br/wp-content/uploads/2009/10/Decreto\\_44864.pdf](https://cdn.sertaobras.org.br/wp-content/uploads/2009/10/Decreto_44864.pdf)

813 Nicolai, B. M., Beullens, K., Bobelyn, E., Peirs, A., Saeys, W., Theron, K. I., & Lammertyn,  
814 J. (2007). Nondestructive measurement of fruit and vegetable quality by means of NIR  
815 spectroscopy: A review. *Postharvest Biology and Technology*, 46(2), 99–118.  
816 <https://doi.org/10.1016/j.postharvbio.2007.06.024>

817 Pasquini, C. (2018). Near infrared spectroscopy: A mature analytical technique with new  
818 perspectives – A review. *Analytica Chimica Acta*, 1026, 8–36.  
819 <https://doi.org/10.1016/j.aca.2018.04.004>

820 Osborne, B. G., Fearn, T., & Hindle, P. H. (1993). *Practical NIR spectroscopy with*  
821 *applications in food and beverage analysis*. Harlow, UK: Longman Scientific and  
822 Technical.

823 Reis, M. G., Agnew, M., Jacob, N., & Reis, M. M. (2022). Comparative evaluation of  
824 miniaturized and conventional NIR spectrophotometer for estimation of fatty acids in  
825 cheeses. *Spectrochimica Acta Part A: Molecular and Biomolecular Spectroscopy*, 279,  
826 121433. <https://doi.org/10.1016/j.saa.2022.121433>

- 827 Rio Grande do Sul (2023). Regulamento Técnico de Identidade e Qualidade do Queijo  
828 Colonial Artesanal. Instrução Normativa no 02 de 24 de fevereiro de 2023, Pub. L. No.  
829 02, Diário Oficial do Rio Grande do Sul. Retrieved april 14, 2023 from:  
830 <https://www.diariooficial.rs.gov.br/materia?id=837948>
- 831 Sant'Ana, A.M.S., Bessa, R.J.B., Alves, S.P., Medeiros, A.N., Costa, R.G., Sousa, Y.R.F., Bezerril,  
832 F.F., Batista, A.S.M., Madruga, M.S., Queiroga, R.C.R.E. Fatty acid, volatile and sensory  
833 profiles of milk and cheese from goats raised on native semiarid pasture or in confinement. *Int.*  
834 *Dairy J.*, 91 (2019), pp. 147-154, 10.1016/j.idairyj.2018.09.008
- 835 Santos, L. S., Cardozo, R. M. D., Nunes, N. M., Inácio, A. B., Pires, A. C. dos S., & Pinto, M.  
836 S. (2017). Easy classification of traditional Minas cheeses using artificial neural  
837 networks and discriminant analysis. *International Journal of Dairy Technology*, 70(4),  
838 492–498. <https://doi.org/10.1111/1471-0307.12370>
- 839 Silva, L. K. R., Cardim de Jesus, J., Vieira Onelli, R. R., Conceição, D. G., Santos, L. S., &  
840 Barbosa Ferrão, S. P. (2023). Spectroscopy (MIR), chromatography (RP-HPLC) and  
841 chemometrics applied to soluble peptides to discriminate the geographic origin of  
842 coalho cheese. *Biocatalysis and Agricultural Biotechnology*, 50, 102678.  
843 <https://doi.org/10.1016/j.bcab.2023.102678>
- 844 Stocco, G., Cipolat-Gotet, C., Ferragina, A., Berzaghi, P., & Bittante, G. (2019). Accuracy  
845 and biases in predicting the chemical and physical traits of many types of cheeses using  
846 different visible and near-infrared spectroscopic techniques and spectrum intervals.  
847 *Journal of Dairy Science*, 102(11), 9622–9638. <https://doi.org/10.3168/jds.2019-16770>